# On Some Characteristics of Ti Oxynitrides Obtained by Pulsed Magnetron Sputtering

Mariana Braic,* Viorel Braic, Mihai Balaceanu, Adrian Kiss, Cosmin Cotrut, Paula Drobe, Alina Vladescu, Cora Vasilescu

$TiO_xN_y$ coatings were investigated as possible candidates for ion diffusion barrier layers. The elemental and phase composition, texture, hardness, adhesion, and corrosion resistance of the coatings were analyzed. The ion release in Ringer solution for uncoated and coated samples were also determined. The film properties were found to significantly depend on the reactive gas composition ($O_2/N_2$ ratio). The coatings proved to enhance the corrosion protection and to reduce the ion release of the uncoated specimens.

## Introduction

In the last few years, thin films of many transition metal oxynitrides such as Ti oxynitrides have gained increasing importance in various applications due to their excellent combination of high hardness, chemical stability, optical and electrical properties, wear and corrosion resistance.[1–3] For example, oxygen-rich $TiN_xO_y$ films have been used as insulating layers in metal–insulator–metal (MIM) capacitive structures in order to avoid oxide interface layer formation, while nitrogen-rich films have been utilized as excellent diffusion barriers.

The goal of the current work is to investigate the effect of the gas composition ($O_2/N_2$ ratio) on some characteristics of $TiO_xN_y$ coatings deposited in a pulsed reactive magnetron sputtering system. The coatings were analyzed in terms of elemental and phase composition, morphology, microhardness, adhesion, and corrosion characteristics. Special attention was devoted to the film protection against corrosion. Ions leached from the substrates during the corrosion test were determined to assess the efficiency of the coating to prevent the diffusion from the substrate. This diffusion barrier effect of these coatings is of utmost importance for biomedical applications.[4] Since the Ni ion release from the biomedical implants in the body fluids is a problem of special interest, the corrosion tests were carried out on pure nickel.

M. Braic, V. Braic, M. Balaceanu, A. Kiss, A.Vladescu
National Institute for Optoelectronics, POB – MG 05, Ro-77125, Magurele, Bucharest, Romania
E-mail: mbraic@inoe.inoe.ro
C. Cotrut, A. Vladescu
Politehnica University of Bucharest, 313 Spl. Independentei, JK 106, Ro-74204, Bucharest, Romania
P. Drob, C. Vasilescu
Institute of Physical Chemistry "I.G. Murgulescu", 202 Spl. Independentei, RO-6002, Bucharest, Romania

## Experimental Part

$TiO_xN_y$ thin films were deposited on Si, Ni, alumina, and high-speed steel substrates, using the reactive pulsed magnetron sputtering method. The experimental set-up has been described elsewhere.[5] The titanium oxynitride coatings were deposited in an $O_2 + N_2$ gas mixture from a metallic Ti (purity 99.9%) cathode. The Ti cathode was fed using a pulsed bipolar generator — type ENI RPG5 (positive pulse length 1.9 μs; repetition rate 100 kHz), to avoid the problems related to the target poisoning and arcing during reactive deposition. The samples were ultrasonically cleaned with acetone and ethanol before deposition; the Ti target was pre-sputtered in a pure argon atmosphere for 5 min in order to clean the surface of the target. The magnetron current and the $N_2$ mass flow rate were kept constant at 3 A and 4 sccm, respectively, while $O_2$ mass flow rate was varied in the range of 0–6 sccm. A negative DC voltage of 60 V was applied on the substrates. For the investigated coatings, the $O_2/N_2$ flow rate ratios were 0, 1/4, 3/4, 1, 5/4, and 3/2. The overall thickness of the coatings was controlled to be of about 2 μm.

Chemical composition of the films was determined by X-ray Photoelectron Spectroscopy (XPS). The XPS spectra were obtained



DOI: 10.1002/ppap.200730605

with a VG ESCA 3 MK II spectrometer using monochromatized Al $K_\alpha$ radiation (1486.6 eV). The spectra were processed using Spectral Data Processor v 2.3 software.

X-Ray diffraction (XRD), with Cu$K_\alpha$ radiation, was carried out to identify the phase composition of the films deposited on alumina substrates.

Vickers microhardness measurements were performed with a microhardness tester at 10 g load. Film thickness was determined by microscope examination of the cross-section through the coating. Scratch tests under standard conditions were undertaken (indenter, 0.2 mm radius diamond tip; load, continuous increase from 0 to 100 N; scratching speed, 10 mm $\cdot$ min$^{-1}$; scratching distance, 10 mm) to determine the coating adhesion. The critical load ($L_c$) values were determined by optical microscopy, $L_c$ being defined as the load where film flaking starts.

The corrosion tests were carried out on coated Nickel substrates. Cylindrical samples (ø10 mm $\times$ 20 mm) were used, coated on the entire surface. The experiments were performed in Ringer solution with the composition (g/l): NaCl, 6.8; KCl, 0.4; $CaCl_2$, 0.2; $MgSO_4 \cdot 7H_2O$, 0.2048; $NaH_2PO_4 \cdot H_2O$, 0.143; $NaHCO_3$, 2.2; glucose, 1, at 25 °C temperature. The electrochemical cell contained a central inlet for the electrode assembly, a cylindrical platinum grid as counterelectrode and a Luggin probe connected with a saturated calomel reference electrode (SCE). Electrochemical, cyclic, potentiodynamic and Tafel polarization techniques were used. Cyclic potentiodynamic polarization was performed starting from the open circuit potential to +0.8 V, with a scan rate of 10 mV $\cdot$ s$^{-1}$, using a Voltalab 80 system with analysis corrosion Voltamaster 4 software. The main electrochemical parameters were determined: $E_{i=0}$, corrosion potential; $E_p$, passivation potential at which the current density is constant; $\Delta E_p$, passive potential range of constant current; $E_b$, breakdown (pitting) potential when the current density increases; $E_{pp}$, pitting protection potential at which the current density on the negative sweep equals the passive current density; $R_p$, polarization resistance. Tafel polarization was applied for $\pm$0.2 V around the corrosion potential ($E_{i=0}$), with a scan rate of 10 mV $\cdot$ s$^{-1}$. Corrosion current densities ($i_{corr}$), corrosion rates and ion release were determined.

*Table 1.* The phases and the corresponding binding energies (BE) of a $TiO_xN_y$ coating.

| Line BE | | Phases |
|---|---|---|
| eV | | |
| Ti2p$_{3/2}$ | Ti2p$_{1/2}$ | |
| 456.3 | 461.3 | TiON species |
| 457.8 | 463.1 | Ti-O suboxides |
| 459.4 | 465.1 | $TiO_2$ |
| O1s | | |
| 530.9 | | TiON species |
| 531.5 | | Ti oxides |
| 533.2 | | Oads, C–O, $H_2O$ |
| N1s | | |
| 397.3 | | TiON species |
| 398.7 | | TiON species |
| 400.5 | | N-O in TiN coatings |

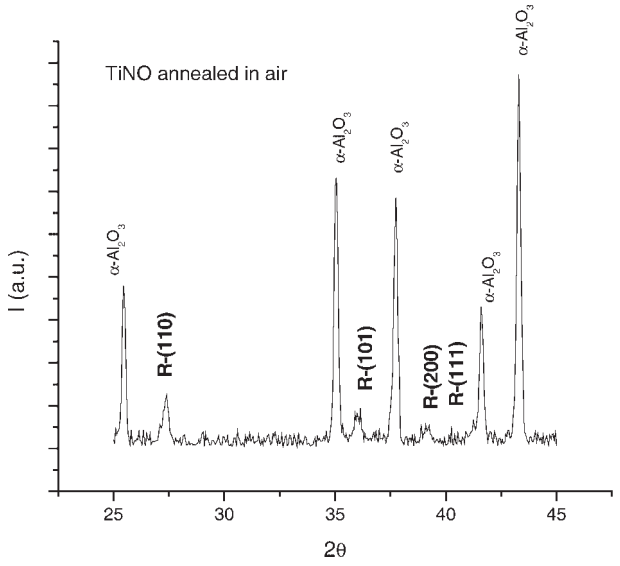


*Figure 1.* XRD spectrum for an annealed TiON film on alumina substrate.

## Results and Discussion

### Microchemical, Microstructural, and Mechanical Properties

The elemental compositions of the $TiO_xN_y$ films were determined from Ti 2p, O 1s, and N 1s peaks. As an example, for a sample prepared with $O_2/N_2 = 1$, the phases detected by peak deconvolution and the corresponding binding energies are summarized in Table 1. According to the literature data,[6–8] the Ti 2p peaks were associated with TiON species, TiO suboxides and $TiO_2$ as follows: Ti 2p$_{3/2}$ (456.3 eV) and Ti 2p$_{1/2}$ (461.3 eV) to TiON; Ti 2p$_{3/2}$ (457.8 eV) and Ti 2p$_{1/2}$ (463.1 eV) to Ti-O suboxides; Ti 2p$_{3/2}$ (459.4 eV) and Ti 2p$_{1/2}$ (465.1 eV) to $TiO_2$. Considering the O 1s spectra, three oxygen peaks were identified at the energies of 530.9 eV (attributed to TiON species), 531.5 eV

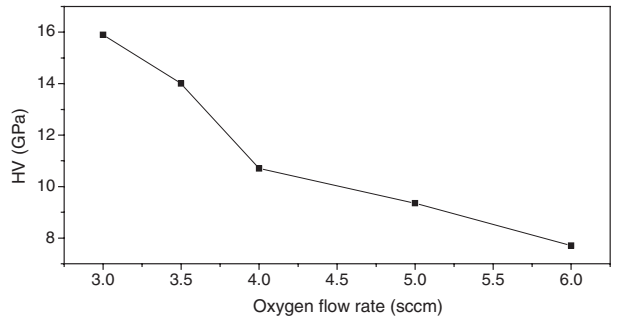


*Figure 2.* TiON coating microhardness vs. oxygen mass flow rate.



DOI: 10.1002/ppap.200730605

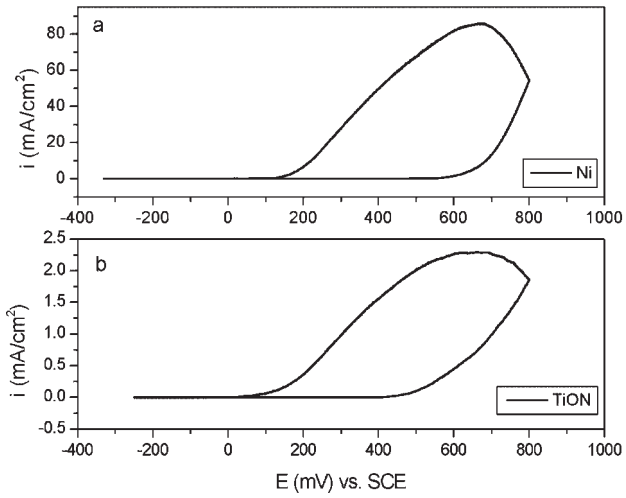


*Figure 3.* Cyclic voltammogram in Ringer solution: (a) Ni and (b) $TiO_xN_y$ ($O_2/N_2 = 1$).

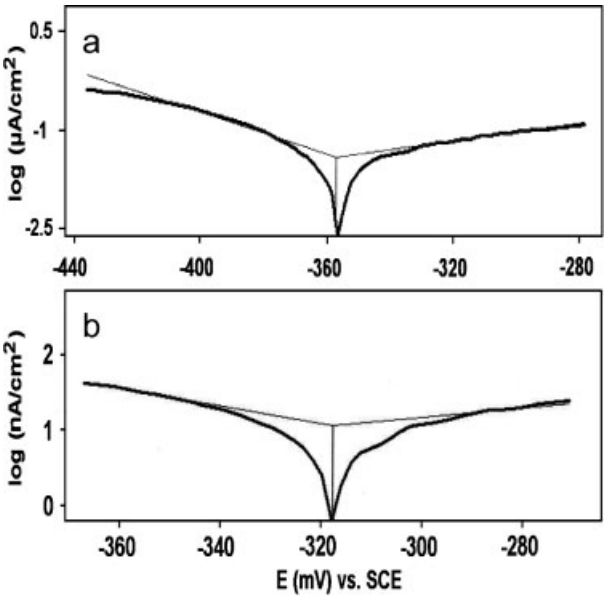


*Figure 4.* Tafel curves in Ringer solution at 25 °C for: (a) Ni and (b) $TiO_xN_y$ ($O_2/N_2 = 1$).

(Ti oxides), 533.2 eV ($O_{ads.}$, C–O and $H_2O$). As for the N 1s spectra, the detected peaks could be assigned to TiON species (397.3 and 398.7 eV), and N-O bonds in TiN coatings (400.5 eV).

It can be seen that the $TiO_xN_y$ films consist of a mixture of titanium oxynitride species, titanium oxides (TiO, $Ti_2O_3$, and $TiO_2$), together with some amount of adsorbed $O_2$, $H_2O$, and COOH. One may note that the ratios of ($O_2 + N_2$) content to Ti content were found to be close to 2, as previously reported for the $TiO_xN_y$ coatings with high O concentrations.[9] With increasing $O_2$ flow rate (at constant magnetron current and $N_2$ flow rate), an increase of the oxygen and titanium contents, together with a decrease of the nitrogen content, were observed.

X-Ray structural analysis revealed that the $TiO_xN_y$ films were amorphous. In the absence of oxygen, the XRD spectrum revealed only the diffraction lines belonging to Ti phase [lines (010), (002), and (011)], since nitrogen content is too low (~30%) for TiN compound synthesis. After annealing in air at 825 K for 5 min the spectra of TiON films revealed a rutile (R) type structure (Figure 1).

Coating microhardness and adhesion were measured for coatings deposited on high-speed steel substrates. Dependence of the Vickers microhardness on the oxygen mass flow rate can be examined in Figure 2. As expected, the microhardness decreases with increasing oxygen flow rate (from 16 to 8 GPa). From the adhesion measurements, critical loads ($L_c$) in the range of 24–32 N were obtained. A slight decrease of the $L_c$ values with oxygen content increase was also observed.

## Electrochemical Corrosion

Typical anodic cyclic voltammograms of Ni substrate uncoated and coated with $TiO_xN_y$, are shown in Figure 3. In Table 2, the main electrochemical parameters in Ringer solution for uncoated and coated samples (with $TiO_xN_y$ or TiN), are presented. The corrosion potentials ($E_{i=0}$) of the coatings are lower than those of the bare metal, as a result of the beneficial barrier effect of the coatings. Passive potential ranges ($\Delta E_p$) of coatings are about equal with those of nickel. Passive current densities are 100–200 times smaller for coated nickel than for bare nickel, revealing the favorable influence of the deposited films on the nickel substrate.

*Table 2.* Main electrochemical parameters in Ringer solution at 25°C.

| Materials | $E_{i=0}$ | $E_p$ | $\Delta E_p$ | $E_b$ | $E_{pp}$ | $\lvert E_{i=0} - E_b \rvert$ | $\lvert E_b - E_{pp} \rvert$ | $i_p$ |
|---|---|---|---|---|---|---|---|---|
| | V | V | V | V | V | V | V | $\mu A \cdot cm^{-2}$ |
| Ni | −0.361 | −0.361 | 0.897 | 0.536 | 0.150 | 0.897 | 0.386 | 1500 |
| Ni + TiN | −0.358 | −0.358 | 0.893 | 0.535 | 0.080 | 0.438 | 0.615 | 11.5 |
| Ni + $TiO_xN_y$ | −0.318 | −0.318 | 0.743 | 0.425 | −0.011 | 0.743 | 0.436 | 4 |

*Table 3.* Corrosion rates and ion release in Ringer solution at 25 °C.

| Materials | $R_p$ | $i_{corr}$ | Corrosion rate | Ion release |
|---|---|---|---|---|
| | $\Omega \cdot cm^{-2}$ | $\mu A \cdot cm^{-2}$ | $mm \cdot year^{-1}$ | $mg \cdot cm^{-2}$ |
| Ni | $2.13 \times 10^{2}$ | $7.6 \times 10^{-2}$ | $0.82 \times 10^{-3}$ | 83.3 |
| Ni + TiN | $6.57 \times 10^{4}$ | $12 \times 10^{-2}$ | $1.29 \times 10^{-3}$ | 131.1 |
| Ni + $TiO_xN_y$ | $1.68 \times 10^{6}$ | $10 \times 10^{-2}$ | $0.11 \times 10^{-3}$ | 11.2 |

For all samples, pitting corrosion was registered. The breakdown potential ($E_b$) had noble values for nickel and $TiO_xN_y$ coatings. Also, for these coatings the pitting protection potentials ($E_{pp}$) show good values; below this potential no pit can be initiated. The ability to repassivation of the pits, quantified by the values of the pitting corrosion resistance ($|E_b - E_{pp}|$) are not very good both for nickel and the coatings. Though, the pitting corrosion tendency is reduced; the high value of the difference $|E_b - E_{pp}|$ indicates a lower tendency to pitting corrosion.

From Tafel curves (Figure 4), corrosion current densities, corrosion rates, and ion release were determined (Table 3). Taking into account all the electrochemical parameters and corrosion rates, it can be concluded that the $TiO_xN_y$ coatings present good protective properties in Ringer solution. Comparing the corrosion rates of $TiO_xN_y$ coated nickel with those of the bare nickel and of the TiN films, it appears that the $TiO_xN_y$ coatings present the lowest values and consequently the best corrosion resistance. Also, the ion release in Ringer solution is minimum for the $TiO_xN_y$ coated Ni substrate.

## Conclusion

$TiO_xN_y$ coatings were successfully deposited on Si, Ni, and high-speed steel substrates using the pulsed reactive magnetron sputtering technique. The $TiO_xN_y$ films were amorphous, with the ratio of the elemental concentrations (N + O)/Ti of about 2. The XPS analysis of the $TiO_xN_y$ films were determined from Ti 2p, O 1s, and N 1s peaks. The $TiO_xN_y$ films consist of a mixture of titanium oxynitride species, titanium oxides (TiO, $Ti_2O_3$, and $TiO_2$), together with some amount of adsorbed $O_2$, $H_2O$, and COOH. Both microhardness and adhesion of the coatings became worse with the increase of the oxygen flow rate. The corrosion behavior was improved by thin film deposition. The corrosion tests on coated Ni also revealed that the titanium oxynitride films were an efficient diffusion barrier for ion release from the substrate. All the tested samples exhibited self-passivation and a low tendency to pitting corrosion.

Acknowledgements: The work was supported under the Project CEEX nos. 25/3.10.2005 and 235/1.08.2006.

Received: September 5, 2006; Revised: December 11, 2006; Accepted: December 14, 2006; DOI: 10.1002/ppap.200730605

Keywords: corrosion resistance; hardness; pulsed magnetron deposition; $TiO_xN_y$ coatings

[1] R. W. Y. Poon, J. P. Y. Ho, X. Liu, C. Y. Chung, P. K. Chu, K. W. K. Yeung, W. W. Lu, K. M. C. Cheung, *Thin Solid Films* **2005**, *488(1–2),* 20.
[2] W. L. Hill, E. M. Vogel, V. Misra, P. K. McLarty, J. J. Wortman, *IEEE Trans. Electron Devices* **1996**, *43,* 15.
[3] E. Alves, A. Ramos, N. Barradas, F. Vaz, P. Cerqueira, L. Rebouta, U. Kreissig, *Surf. Coat. Technol.* **2004**, *180-181,* 372.
[4] L. B. Dalmau, H. C. Alberty, J. S. Parra, J. Prosthet, *Dental* **1984**, *52,* 116.
[5] M. Braic, M. Balaceanu, A. Purice, F. Stokker-Cheregi, A. Moldovan, N. Scarisoreanu, G. Dinescu, A. Dauscher, M. Dinescu, *Surf. Coat. Technol.* **2006**, *200,* 6505.
[6] Ju. F. Huralev, M. V. Kuznetsov, V. A. Gubanov, *J. Elect. Spectro. Relat. Phenom.* **1992**, *38,* 169.
[7] T. Tataeishi, Y. Ito, Y. Okazaki, *Mater. Trans., JIM* **1997**, *38,* 78.
[8] Ch. Cardinaud, G. Lemperiere, M. C. Peignon, P. Y. Jouan, *Appl. Surf. Sci.* **1993**, *68,* 595.
[9] P. G. Wu, C. H. Ma, J. K. Shang, *Appl. Phys.* **2005**, *A81,* 1411.



DOI: 10.1002/ppap.200730605